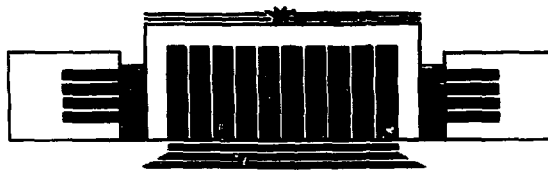S.I. Dolinsky, V.P. Druzhinin, M.S. Dubrovin,
V.B. Golubev, V.N. Ivanchenko, A.P. Lysenko,
A.A. Mikhailichenko, E.V. Pakhtusova, A.N. Peryshkin,
S.I. Serednyakov, Yu.M. Shatunov, V.A. Sidorov

RADIATIVE DECAYS
OF ρ AND ω MESONS

IYaF--88-89.

Institute of Nuclear Physics

S.I. Dolinsky, V.P. Druzhinin, M.S. Dubrovin,
V.B. Golubev, V.N. Ivanchenko, A.P. Lysenko,
A.A. Mikhailichenko, E.V. Pakhtusova, A.N. Peryshkin,
S.I. Serednyakov, Yu.M. Shatunov, V.A. Sidorov

RADIATIVE DECAYS
OF ρ AND ω MESONS

Radiative Decays of ρ and ω Mesons

S.I.Dolinsky, V.P.Druzhinin, M.S.Dubrovin,
V.B.Golubev, V.N.Ivanchenko, A.P.Lysenko,
A.A.Mikhailichenko, E.V.Pakhtusova, A.N.Peryshkin.
S.I.Serednyakov, Yu.M.Shatunov, V.A.Sidorov

Institute of Nuclear Physics
630090, Novosibirsk, USSR

ABSTRACT

The results of the measurements of radiative decays of ρ and ω mesons with the Neutral Detector at e^+e^- collider VEPP-2M are presented. The branching ratio of the decay $\omega \to \pi^0\gamma$ was measured with higher than in previous experiments accuracy:

$$B(\omega \to \pi^0\gamma) = 0.089 \pm 0.006.$$

The $\rho^0 \to \pi^0\gamma$ branching ratio was measured for the first time:

$$B(\rho^0 \to \pi^0\gamma) = (7.9 \pm 2.0) \cdot 10^{-4}.$$

The decays $\rho, \omega \to \eta\gamma$ were studied. Their branching ratios with the assumption of constructive $\rho - \omega$ interference are:

$$B(\omega \to \eta\gamma) = (7.3 \pm 2.9) \cdot 10^{-4},$$
$$B(\rho \to \eta\gamma) = (4.0 \pm 1.1) \cdot 10^{-4}.$$

The branching ratios of $\omega \to \pi^+\pi^-\pi^0$ and $\omega \to e^+e^-$ decays were also measured:

$$B(\omega \to \pi^+\pi^-\pi^0) = 0.894 \pm 0.006,$$
$$B(\omega \to e^+e^-) = (7.14 \pm 0.36) \cdot 10^{-5}.$$

The upper limit of the $\omega \to \pi^0\pi^0\gamma$ branching ratio was placed:

$$B(\omega \to \pi^0\pi^0\gamma) < 4 \cdot 10^{-4} \text{ at } 90\% \text{ confidence level.}$$

1. INTRODUCTION

The radiative decays of ω, ρ, and other light vector mesons are a good probe to investigate the quark content and the interaction between constituent quarks inside mesons. The partial widths of these decays are predicted by quark model [1], but the detailed analysis of the experimental results and different theoretical models (see review [2]) leaves several quiestions requiring an improvement of experimental accuracy.

The $\omega \to \pi^0 \gamma$ branching ratio was measured in many experiments and its table value has an accuracy of 6% [3]. However this result was obtained by averaging the results of several experiments, the most precise of which had an error of 15%. The branching ratios of $\rho, \omega \to \eta \gamma$ were measured in the only experiment in the reaction of diffractive photoproduction [4]. The decay $\rho \to \pi \gamma$ was also studied, but only for charged ρ^- in experiments using Primakoff-effect, where higher than 10% accuracy was achieved [5, 6]. The decay of neutral ρ^0 meson $\rho^0 \to \pi^0 \gamma$ has not been observed yet.

This work continues the sequence of experiments on the radiative decays of vector mesons [7, 8]. The measurements of following decays are presented:

$$\omega \to \pi^0 \gamma , \tag{1}$$

$$\rho^0 \to \pi^0 \gamma , \tag{2}$$

$$\omega \to \eta \gamma , \tag{3}$$

$$\rho^0 \to \eta \gamma . \tag{4}$$

3

The results were obtained using the reactions:

$$e^+e^- \to \rho, \omega \to \pi^0\gamma \to \gamma\gamma\gamma \ , \tag{5}$$

$$e^+e^- \to \rho, \omega \to \eta\gamma \to \gamma\gamma\gamma \ , \tag{6a}$$

$$\to \pi^0\pi^0\pi^0\gamma \to 7\gamma \ . \tag{6b}$$

The upper limit of the probability of the decay

$$\omega \to \pi^0\pi^0\gamma \tag{7}$$

was placed.

The experiment was performed at e^+e^- collider VEPP-2M [9] with the Neutral Detector [10], which is based on NaI(Tl) electromagnetic calorimeter of a mass of 2.6 tons. The total integrated luminosity of 5.3 pb^{-1} was accumulated in the energy range $2E = \sqrt{s} = 0.5 \div 1.0$ GeV.

In the Chapters 2−4 the analysis of the reactions (5) and (6a) in the 3γ final state is presented. In the Chapter 5 the reaction (6b) is analysed. The Chapter 6 is devoted to multiphoton background processes and a search for the reaction (7). In the Chapter 7 the results in terms of branching ratios and partial widths are presented. In the last Chapter 8 a brief comparison of our results with the results of other experiments and the predictions of quark model is done.

2. REACTION $e^+e^- \to \rho, \omega \to \pi^0(\eta)\gamma \to \gamma\gamma\gamma$. EVENT SELECTION

For an event to be accepted as a candidate of the processes (5) or (6a), it had to satisfy following conditions. The event must contain 3 photons in the calorimeter, and the energy-momentum balance must hold within experimental accuracy. To suppress the background from $e^+e^- \to 2\gamma$, when one of the photons splits into two due to shower fluctuations in the calorimeter, the requirements were set on the minimal spatial angle between any two particles to be greater than 30 degrees and the energy of any photon to be within the interval from 30 MeV to the beam energy E. The further selection was performed with the use of kinematic fit [11]. The total of 10625 events were found satisfying the selection criteria and kinematic fit. The sample contained events of the processes (5), (6a) as well as background events of the 3γ annihilation:

$$e^+e^- \to \gamma\gamma\gamma \ (QED). \tag{8}$$

4

The final separation between the reactions (5), (6a) and **(8)** was performed using the differences in recoil mass distributions. To this end the recoil mass of each photon was calculated:

$$m_i = \sqrt{s - 2\omega_i\sqrt{s}},$$

where ω_i is a photon energy. In Fig. 1,a,b,c the Dalitz plots are shown for the Monte Carlo simulated events of the reactions (5), (6a) and (8) at $\sqrt{s}$ close to ω meson mass. The dashed lines show the kinematical bounds determined by energy-momentum conservation. As can be seen in Fig. 1,b, the events of the process (5) are concentrated around the line corresponding to $m_{min} = m_{\pi^0}$. This is also valid for the whole energy range of the collider. The most of the events of the reaction (6a) are concentrated around the $m_{max} = m_\eta$ line (Fig. 1,c). But since the η meson mass is comparable with the total energy of events, this picture varies with the energy of the collider. The population density of the Dalitz plot for the reaction (8) is smooth (Fig. 1,a). The distribution of the experimental events within the energy range $2E = m_\omega \pm 3$ MeV is shown in Fig. 1,d. The contributions of the processes (5) and (8) are clearly visible, while the process (6a) is completely obscured by the background due to the reaction (8). However the distribution over maximal recoil mass for events with $m_{min} > 250$ MeV (Fig. 2) shows a peak at the η meson mass which indicates the existence of the decay (3). In the Fig. 3 the distribution over m_{min} for experimental and simulated events of the reaction (5) is shown. The experiment and Monte Carlo simulation are in a good agreement. Considering the distributions over recoil mass the following criteria were set for separation of the events between the processes (5), (6a), and **(8)**. If any recoil mass in an event fell within an interval $80 - 190$ MeV, corresponding to π^0 meson mass, than this event was ascribed to the reaction (5). In order to suppress this process when events of the processes (6a) and (8) were selected, the requirement $m_{min} > 200$ MeV was set. To investigate the reaction (6a) the events with one of the recoil masses being within the interval of $520 - 580$ MeV corresponding to η meson were selected. Remaining events were ascribed to the process (8). The experimental detection cross sections of the processes (5), (6a), (8) with the selection criteria described above are shown in Fig. 4 as a function of energy.
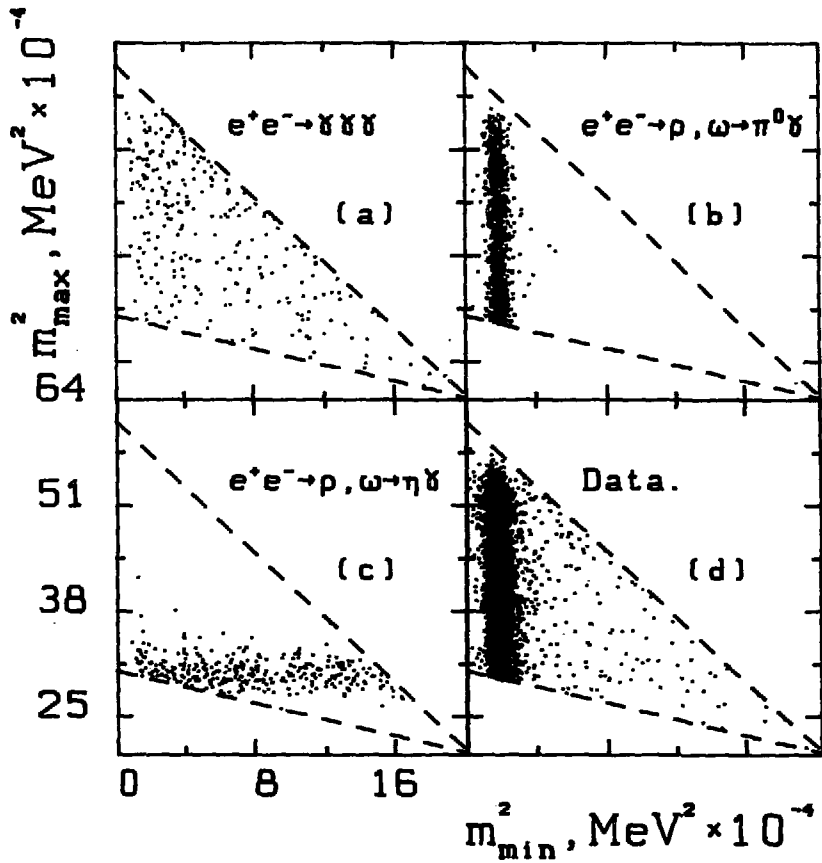
Fig. 1. Scatterplots over the m_{min}^2 and m_{max}^2. m_{max} and m_{min} are the maximal and minimal recoil masses of the photons in an event. *a, b, c*—Monte Carlo simulation of $\gamma\gamma\gamma$(QED), $\pi^0\gamma$, $\eta\gamma$ final states respectively. The center of mass energy is equal to ω meson mass. *d*—Experimental events from the center-of-mass energy interval 779—785 MeV.
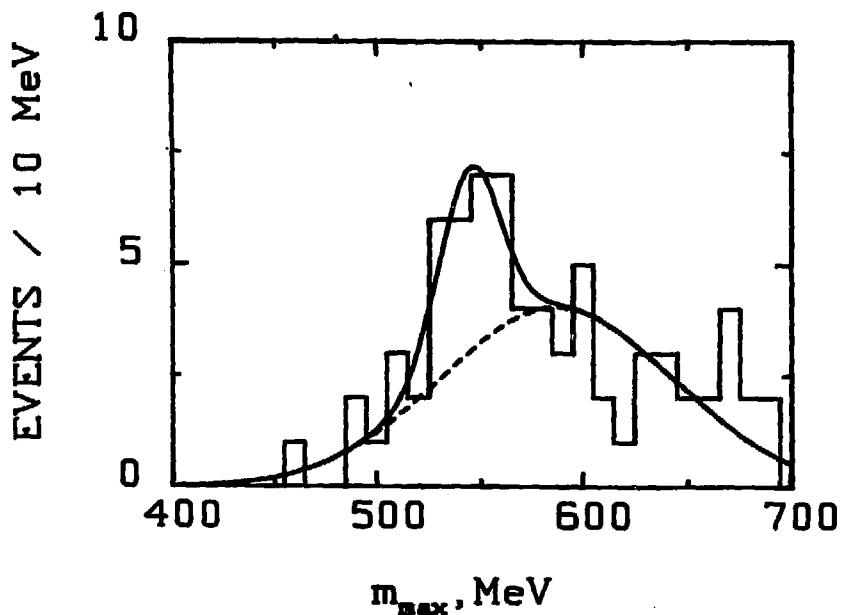
Fig. 2. Distribution of events over maximum recoil mass at $m_{min} > 250$ MeV. Histogram—experimental events, solid line—the sum of the processes (6a) and (8), dashed line—the contribution of the process (8) alone.
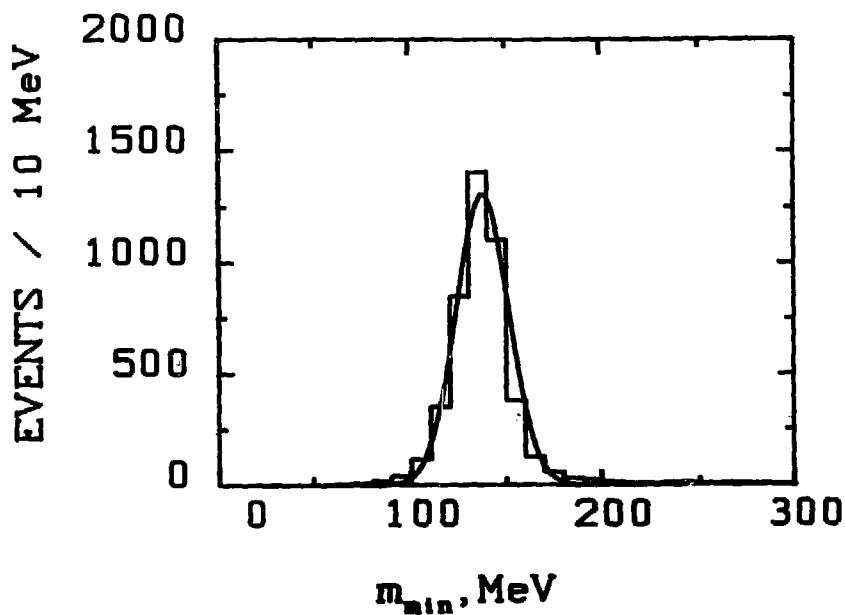

Fig. 3. Distribution of events over minimal recoil mass. Histogram—experimental events, solid line—Monte Carlo simulation of the process (5).

3. CROSS SECTION PARAMETRIZATION

To fit the cross section under the selection criteria of the reaction (8), the following parametrization was used:

$$\sigma^{j}_{e^+e^-\to 3\gamma}(s) = \sigma_{03\gamma}\,\frac{800^2}{s}\,k_j(s)\,\lambda_{3\gamma}(s) \tag{9}$$

where $\sigma^{j}_{e^+e^-\to 3\gamma}(s)$ is a detection cross section of (8) under the selection criteria for the final state j ($j = \pi^0\gamma,\ \eta\gamma,\ \gamma\gamma\gamma$); $\sigma_{03\gamma}$ is a differential cross section of the process (8) at $\sqrt{s} = 800$ MeV, integrated over solid angle for $30° < \theta < 150°$; $k_j(s)$ is a factor taking into account the difference in the contributions of the process (8) for different selection criteria; $\lambda_j(s)$ is a factor allowing for radiative corrections, beam energy spread, and precision of energy setting.

The experimental detection cross sections under the selection criteria for the processes (5) and (6) were approximated as follows:

$$\sigma^{P\gamma}_{vis}(s) = \sigma_{P\gamma}(s)\,\varepsilon_{P\gamma}(s)\,\lambda_{P\gamma}(s) + \sigma^{P\gamma}_{e^+e^-\to 3\gamma}(s)\ ;$$

$$P \equiv \pi^0\ \text{or}\ \eta\ ;$$

$$\sigma_{P\gamma}(s) = |A_\rho + A_\omega(1 + A_{\rho\omega}) + A_\phi|^2; \tag{10}$$

$$A_V = \frac{m_V\,\Gamma_V\,\sqrt{\sigma_0(e^+e^-\to V\to P\gamma)}}{m_V^2 - s - i\sqrt{s}\cdot\Gamma_V(s)}\left(\frac{1 - m_P^2/s}{1 - m_P^2/m_V^2}\right)^{3/2} e^{i\theta_{VP\gamma}}\ ;$$

$$V \equiv \rho,\omega\ \text{or}\ \Phi\ ;\qquad A_{\rho\omega} = \sqrt{\frac{\Gamma_{\rho ee}}{\Gamma_{\omega ee}}}\,\frac{2\,|\delta|e^{i\theta_{\rho\omega}}}{m_\rho^2 - s - i\sqrt{s}\,\Gamma_\rho(s)}\ .$$

Here $\sigma^{P\gamma}_{vis}(s)$ is a detection cross section of the processes (5) and (6a,b); $\sigma_{P\gamma}(s)$ are total cross sections of these processes; $\sigma_0(e^+e^-\to V\to P\gamma)$ is a cross section of the reaction $e^+e^-\to V\to P\gamma$ in the maximum of a resonance V; $\varepsilon_{P\gamma}(s)$ is a detection efficiency for the selection criteria described above, including the branching ratio of the decay $P\to\gamma\gamma$ for the reaction (6a) and $\eta\to3\pi^0$ for the reaction (6b); A_V is an amplitude of the decay $V\to P\gamma$; m_P, m_V, Γ_V are the masses and widths of corresponding resonances; $A_{\rho\omega}$ is an amplitude taking into account $\rho-\omega$ mixing [12] in the transition $\rho\to\omega\to P\gamma$; $|\delta|$ and $\theta_{\rho\omega}$ are the module and phase of the $\rho-\omega$ mixing; $\Gamma_{\rho ee}$, $\Gamma_{\omega ee}$ are the electron widths of ρ and ω mesons. The values of the parameters $k_j(s)$ and $\varepsilon_{P\gamma}(s)$ were calculated with the use of Monte Carlo simulation. The parameters of $\rho-\omega$ mixing were obtained from the experimental data on the decay $\omega\to\pi^+\pi^-$

8

[3] with the application of the model [12]: $|\delta| = 2.3$ MeV, $\theta_{\rho\omega} = 0°$. The value of the ω meson width $\Gamma_\omega = 8.4 \pm 0.1$ MeV was taken from our previous work [13], which had higher accuracy. The phases $\theta_{\omega P\gamma}$ and $\theta_{\Phi P\gamma}$ were set to 0 and 180° respectively. The value of $\sigma_0(e^+e^- \to \Phi \to P\gamma)$ was taken from our previous work [7] on radiative decays of Φ meson. The other constants were set to their table values [3].

4. THREE-PHOTON FINAL STATE ANALYSIS

The fitting of the detection cross section (9) of the process (8) to experimental data yielded the value of $\sigma_{03\gamma} = 10.8 \pm 0.8$ nb which agrees well with the calculated one:

$$\sigma_{03\gamma} = 10.7 \pm 0.1 \text{ nb.} \qquad (11)$$

This means that no other non-resonant background was observed. It should be pointed out that the cross section of (8) (Fig. 4,a) does not show the resonant contribution from the reaction (5). Fitting of the detection cross sections of the processes (5) and (6a) was done further, using the calculated value (11). The experimental data on the reaction (5) allow three possible interpretations for the $\pi^0\gamma$ final state production cross section:

1. only ω meson;
2. ρ and ω mesons, constructive interference ($\theta_{\rho\pi\gamma} \approx 0°$);
3. ρ and ω mesons, destructive interference ($\theta_{\rho\pi\gamma} \approx 180°$);

(the possibility to isolate the unique solution will be discussed later in Chapter 7). In all three cases the approximation included nonresonant background due to reaction (8). The optimum values of the approximation parameters are presented in the Table 1.

Table I

Results of Approximation of Experimental Data.
Optimum Values of Approximation Parameters for Different Interpretations

Model	$\sigma_0(e^+e^- \to \omega \to \pi^0\gamma)$, nb	$\sigma_0(e^+e^- \to \rho \to \pi^0\gamma)$, nb	$\theta_{\rho\pi\gamma}$, degrees	χ^2/n_D
1. ω	$176 \pm 5 \pm 6$	0	0	92/91
2. $\rho + \omega$	$152 \pm 5 \pm 5$	$0.88 \pm 0.18 \pm 0.12$	10 ± 6	61/89
3. $\rho - \omega$	$240 \pm 7 \pm 8$	$6.0 \pm 0.5 \pm 0.6$	168.1 ± 1.6	61/89

9

The first error here is a statistical one, the second is systematic, which includes uncertainties of detection efficiency estimation, luminosity monitoring, and background subtraction. The systematic error of the detection efficiency has been assessed by comparing the distributions of experimental and Monte Carlo simulated events over the parameters used for selection of $\pi^0\gamma$ events. The systematic error of integrated luminosity measurement, which was performed using the reactions $e^+e^- \to e^+e^-$ and $e^+e^- \to \gamma\gamma$, was estimated similarly. The background subtraction error was evaluated by fitting the curve (10) to experimental cross section of the process (5) with the parameter $\sigma_{03\gamma}$ set free. The resulting optimum value $\sigma_{03\gamma} = 11.5 \pm 1.3$ nb is in a good agreement with the theoretical one (11). At the same time the variation of other approximation parameters is insignificant: $\sigma_0(e^+e^- \to \rho \to \pi^0\gamma)$ decreases by 13% and $\sigma_0(e^+e^- \to \omega \to \pi^0\gamma)$ increases by less than 1% in comparison with fitting (10) with fixed theoretical value of $\sigma_{03\gamma}$. The effect of electromagnetic $\rho - \omega$ mixing in the $\pi^0\gamma$ decay causes change of the cross section in the maximum of ω resonance by 2% and shift of $\theta_{\rho\pi\gamma}$ by 6 degrees.

The fitting of the curve (10) to the experimental detection cross section under the selection criteria of the process (6a) (Fig. 4,c) yields the following values of the approximation parameters:

$$\sigma_0(e^+e^- \to \omega \to \eta\gamma) = 1.1^{+1.2}_{-0.8} \text{ nb}, \qquad (12)$$

$$\sigma_0(e^+e^- \to \rho \to \eta\gamma) < 0.6 \text{ nb} \qquad (13)$$

at 90% confidence level. Because of absence of statistically significant contribution of ρ meson, here we have no ambiguity in the fitting, and the result (12) does not depend on the relative phase $\theta_{\rho\eta\gamma}$. More precise results for the decays (3) and (4), based on the analysis of multiphoton final state in the reaction (6b), would be described below.

5. REACTIONS $e^+e^- \to \rho, \omega \to \eta\gamma \to 7\gamma$

In the reaction (6b) η meson decays into $\pi^0\pi^0\pi^0$, and the final state contains 7 photons. Other known decays of ρ and ω do not produce multiphoton events (see Chapter 6), so we suppose that the reaction (6b) is the only source of such events.

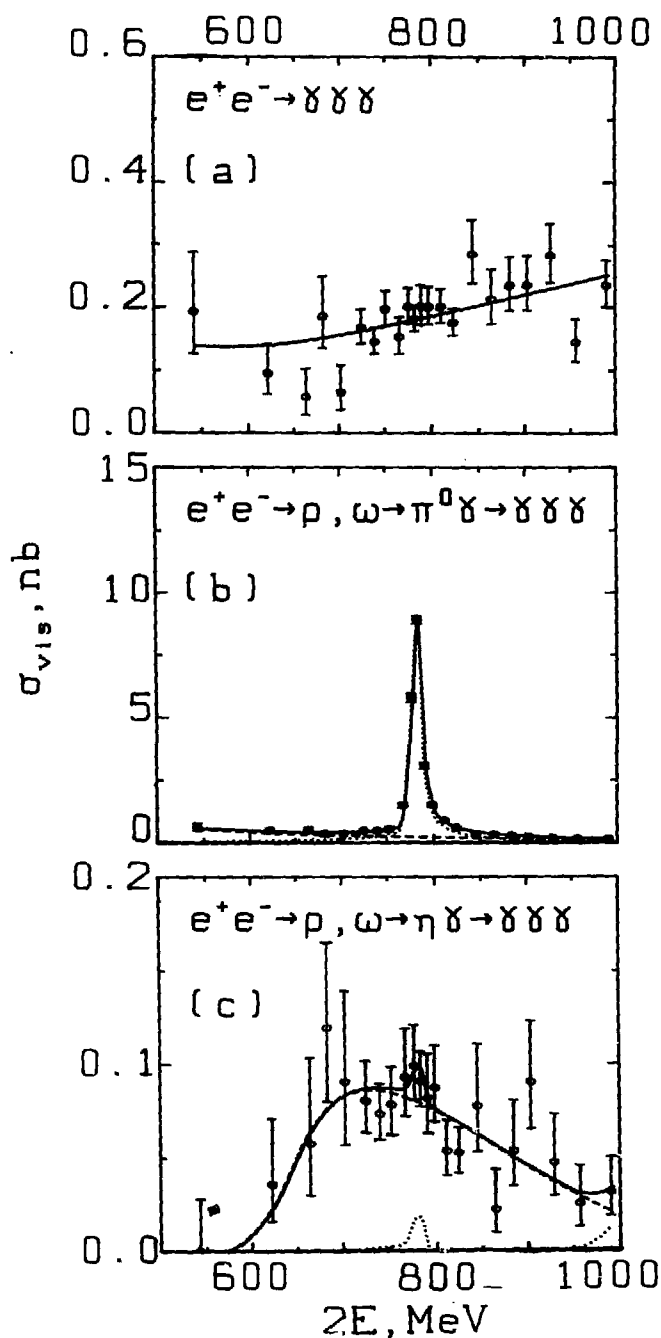Because of incomplete coverage of the solid angle by the calori-

Fig. 4. Visible cross section of the processes (8), (5) and (6a). Points—experimental data; solid line—optimal approximation with the use of the formula (10); dashed line represents a contribution from the process (8) calculated using expression (9); dotted line is a resonant contribution from the processes (5) and (6a).

11

meter, some photons may escape detection. Another cause of losing photons is a merge of showers in the detector and a finite energy threshold of the calorimeter. Monte Carlo simulation of the reaction (6b) shows that the most probable number of the detected photons is close to 5. The sample of events with the number of detected photons less than 5 is considerably contaminated by the background events of the reactions (5), (8), and QED process $e^+e^- \to \gamma\gamma\gamma\gamma$ [14]. So only the events with 5 or more photons were selected for further analysis. This sample together with the events of the process (6b) containes the background due to cosmic particles only. To suppress it the following selection criteria were applied.

1. The event must contain at least one π^0, which is a $\gamma\gamma$ pair with the invariant mass of $95 \div 175$ MeV.
2. The minimal spatial angle between any two photons must be greater than $30°$.
3. The energy deposition in the calorimeter must be within the limits from E to $1.6E$.
4. The total transverse momentum $P_\perp$ must be less than $0.2E/c$.
5. The energy of any reconstructed π^0 in an event must be less than 330 MeV.

In the Fig. 5 the recoil mass distribution for the most energetic photon in an event is shown for both experimental and simulated events. The peak is positioned at η meson mass and the experimental distribution agrees well with simulated one. The experimental distributions over $P_\perp$, total energy deposition in the calorimeter, and photon spectra do not contradict the simulated ones. This allows to attribute all the selected events to the process (6b). The detection cross section obtained is shown in Fig. 6 as a function of the beam energy.

The approximation of detection cross section was done with the use of expression (10), without the term taking into account non-resonant contribution from the process (8). As a result two different solutions were obtained (Table 2), corresponding to constructive

Table 2

Approximation of Experimental Data for the Process (6b)

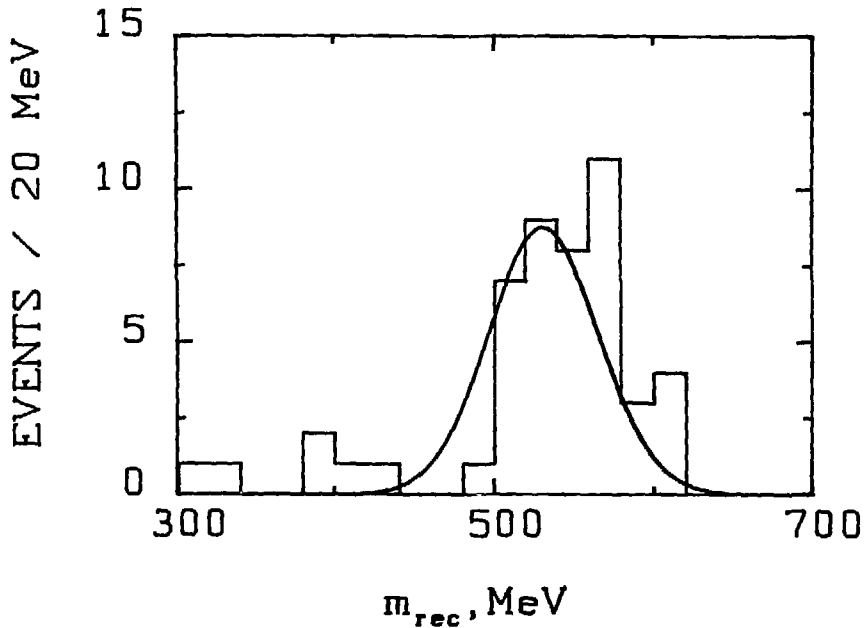| Model	$\sigma_0(e^+e^- \to \omega \to \eta\gamma)$, nb	$\sigma_0(e^+e^- \to \rho \to \eta\gamma)$, nb	$\theta_{\rho\omega}$, degrees
1. $\rho + \omega$	0.45 ± 0.12	1.25 ± 0.5	-17 ± 19
2. $\rho - \omega$	0.81 ± 0.16	6.0 ± 0.9	168 ± 6

12

Fig. 5. Recoil mass spectrum of the most energetic photon in an event for multiphoton events. Histogram—experimental data, solid line—Monte Carlo simulation of the process (6b).
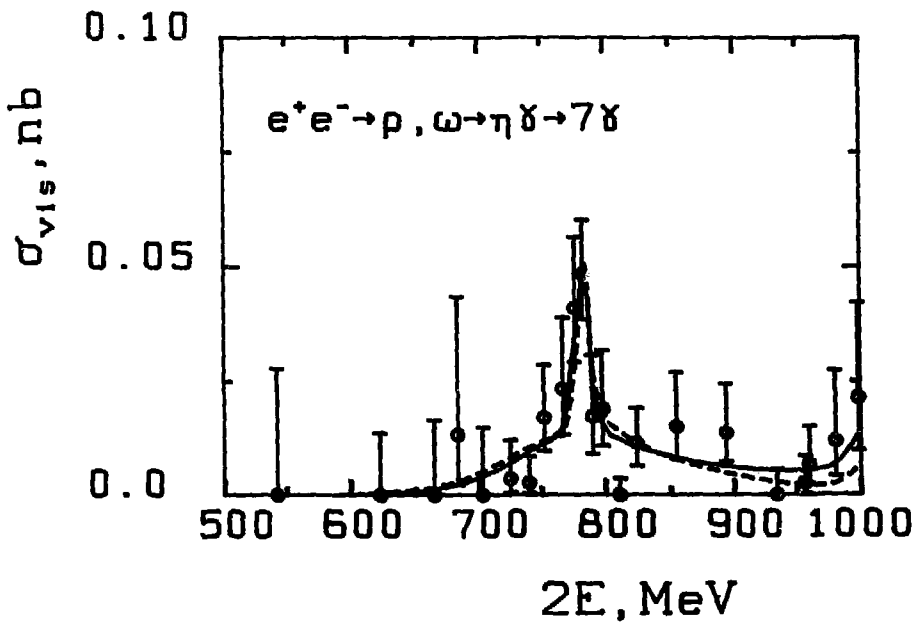

Fig. 6. Visible cross section of the process (6b) in multiphoton mode. Points—experimental data, solid line—optimal approximation with the use of (10) assuming constructive $\rho-\omega$ interference, dashed line—approximation for destructive $\rho-\omega$ interference.

13

and destructive $\rho - \omega$ interference (Fig. 6). We did not approximate the data assuming the absence of the decay (4), because it would require introduction of unknown non-resonant multiphoton process.

6. SEARCH FOR $\omega \rightarrow \pi^0 \pi^0 \gamma$

To estimate background to radiative decays under study we considered different possible processes with multiphoton final states. It may be assumed that such final states are originated by π^0 and η mesons with their subsequent decay into gammas. However, the decays of ω meson into final states consisted only of π^0 and η mesons are forbidden by C parity conservation. Furthermore, with the increase of the number of π^0 and η mesons the final state phase space decreases, thus the corresponding branching ratios decrease too. So the decay (7) seems to be the most probable multiparticle neutral decays of ω meson. This decay might be enhanced by the transition through exotic scalar intermediate states $S(\sigma(400)$, $\varepsilon(700)$, $f_0(975)$, ...), decaying into two π^0: $\omega \rightarrow S\gamma \rightarrow \pi^0 \pi^0 \gamma$. Existing results on the decay (7) [3] are inconsistent, varying from the observation of the decay at 2% branching ratio to upper limit at even lower level.

The events of the decay (7) were selected with the use of selection criteria similar to those explained in Chapter 5. The difference was that the detection of all photons in the decay was required. In this case the total energy deposition in an event must be close to $2E$. The kinematic fit [11] was done with the constraint that two π^0s be present in an event. The total of 16 events were thus selected. 5 of them were collected within the center of mass energy range near ω meson mass. All selected events can be explained in terms of background process (6b). Fitting the sum of Breit — Wigner contribution of ω meson and cross section of the process (6b) with the parameters determined in Chapter 5 to the experimental data, we obtained an upper limit of the cross section in the maximum of ω resonance:

$$\sigma_0(e^+e^- \rightarrow \omega \rightarrow \pi^0 \pi^0 \gamma) < 0.7 \text{ nb} \tag{14}$$

at 90% confidence level.

7. THE RESULTS IN TERMS OF BRANCHING RATIOS AND WIDTHS

We define the branching ratio as follows:

$$B(V \to f) = \sigma_0(e^+e^- \to V \to f) / \sigma_0(e^+e^- \to V \to \text{all}),$$

where σ_0 is a cross section in the maximum of resonance V. The partial width of a decay is defined as a product of branching ratio of the decay and the full width of the vector resonance:

$$\Gamma(V \to f) = \Gamma_V B(V \to f).$$

The width and total cross section of ρ meson production in e^+e^- annihilation were set to their table values [3]. The corresponding values for ω meson used for fitting:

$$\Gamma_\omega = 8.4 \pm 0.1 \text{ MeV},$$

$$\sigma_0(e^+e^- \to \omega \to \pi^+\pi^-\pi^0) = 1530 \pm 84 \text{ nb},$$

were obtained in our previous work [13]. The latter differs by 4% from the result of [13] due to systematic error of the measurement of integrated luminosity. The total cross section of ω meson production at e^+e^- colliding beams has been assumed equal to the sum of partial cross sections: $e^+e^- \to \omega \to \pi^+\pi^-\pi^0$, $\pi^0\gamma$ and $\pi^+\pi^-$. The latter was taken from the tables [3].

The cross sections of the processes under study presented in Tables 1 and 2 are ambiguous. They depend on the model of $\rho - \omega$ interference. As a final result the only physically valid solution must be chosen.

First of all let us consider in detail the solutions obtained for the decays (1) and (2). In Fig. 7 the calculated detection cross sections for each solution from the Table 1 and experimental data are shown with respect to the calculated cross section corresponding to constructive $\rho - \omega$ interference. The experimental data in Fig. 7 were averaged over five energy intervals, which were chosen to maximize the distinction in detection cross sections for different solutions. Fig. 7 shows that agreement between experimental data and approximations is much better for the solutions No.2 and 3 than for the solution No.1, i. e. the contribution from $\rho^0 \to \pi^0\gamma$ decay is statistically significant. However the difference between the solutions No.2 and 3 themselves is less than 2%, so it is not possible to choose the unique solution using only our experimental data. This
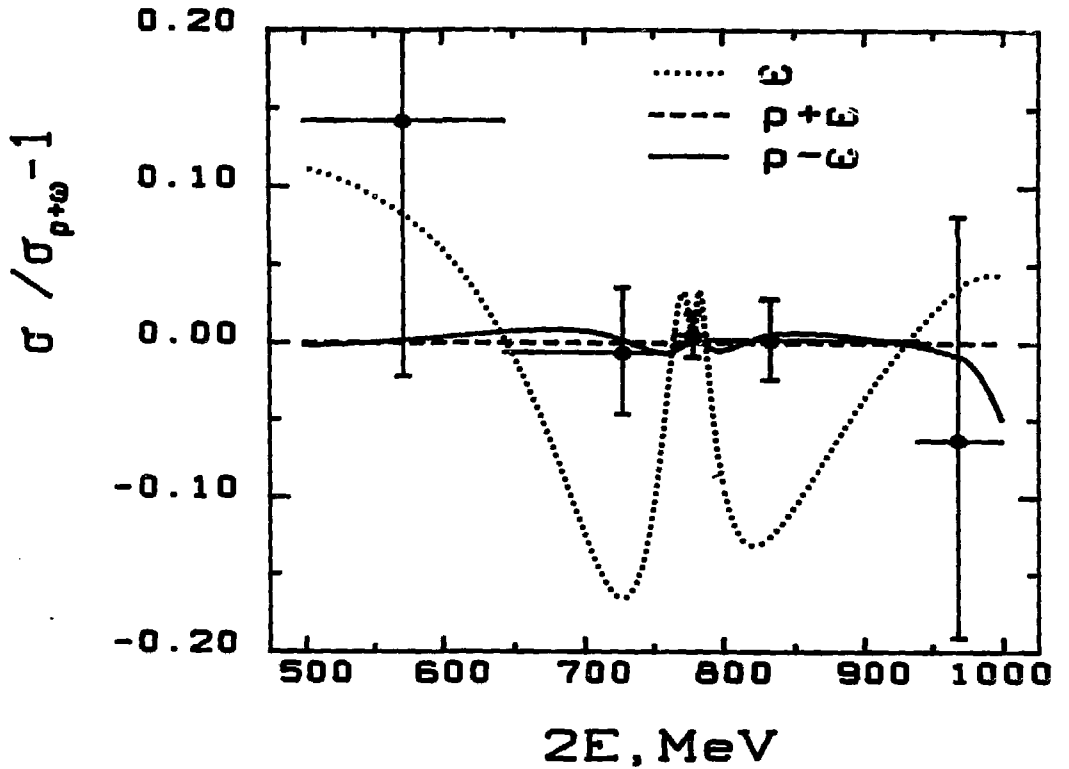
Fig. 7. The approximation of visible cross section of the decays (1) and (2). The relative difference between the different solutions. Solution No.2 has been taken as a base (see Table 2). Dotted line — the relative difference between the solutions No.1 and 2, solid line — the relative difference between the solutions No.3 and 2, the points represent the difference between visible cross section and solution No.2.

becomes feasible if we apply the results of other works, carried out in different technique.

Table 3

Comparison of Different Solutions for $\rho - \omega$ Interference with the Results of Other Experiments

Model	$\Gamma(\rho \to \pi\gamma)$, keV	$B(\omega \to \pi^0\gamma)/B(\omega \to \pi^+\pi^-\pi^0)$
1. ω	0	0.115 ± 0.008
2. $\rho - \omega$	824 ± 116	0.157 ± 0.011
3. $\rho + \omega$	121 ± 31	0.099 ± 0.007
The other experiments		
4. ρ^-	$81 \pm 4 \pm 4$ [6]	—
5. ω	—	0.089 ± 0.013 [15]

Presented in Table 3 are our results for the partial width of the decay $\rho \to \pi\gamma$ and the ratio of branching ratios $B(\omega \to \pi^0\gamma)/B(\omega \to \pi^+\pi^-\pi^0)$ for all three possible cases together with the most accurate experimental results of other groups. In the work [6] the $\rho^- \to \pi^-\gamma$ partial width was measured using Primakoff-effect. Quark model together with isospin invariance predicts that the partial widths of radiative decays of charged and neutral ρ mesons are the same. The decay (1) was studied in the work [15] in the reaction $\pi^- p \to \omega n$. Due to different mechanism of ρ and ω production in this case, the interference between them vanishes. Comparing the results presented in Table 3 one can see that only one solution with constructive $\rho - \omega$ interference do not contradict other experiments.

Another indication of the validity of such a choice is the value of the parameter $\theta_{\rho\pi\gamma}$. Since the electromagnetic $\rho - \omega$ mixing amplitude was included in the formula (10) explicitly, the $\theta_{\rho\pi\gamma}$ must be equal to either 0 or 180 degrees. This condition is satisfied for the solution corresponding to constructive $\rho - \omega$ interference and is not satisfied for destructive interference. Thus our final results corresponding to con tructive interference are:

$$\sigma_0(e^+ e^- \to \omega \to \text{all}) = 1711 \pm 86 \text{ nb},$$

$$B(\omega \to \pi^+\pi^-\pi^0) = 0.894 \pm 0.006,$$

$$B(\omega \to \pi^0\gamma) = 0.089 \pm 0.006,$$

$$B(\rho^0 \to \pi^0\gamma) = (7.9 \pm 2.0) \cdot 10^{-4},$$

$$B(\omega \to e^+e^-) = \frac{M_\omega^2}{12\pi}\sigma_0(e^+e^- \to \omega \to \text{all}) = (7.14 \pm 0.36) \cdot 10^{-5},$$

$$B(\omega \to \pi^0\pi^0\gamma) < 4 \cdot 10^{-4} \text{ at } 90\% \text{ confidence level,}$$

$$\Gamma(\omega \to \pi^+\pi^-\pi^0) = 7.51 \pm 0.10 \text{ MeV,} \tag{15}$$

$$\Gamma(\omega \to e^+e^-) = 0.60 \pm 0.03 \text{ keV,} \tag{16}$$

$$\Gamma(\omega \to \pi^0\gamma) = 746 \pm 51 \text{ keV,} \tag{17}$$

$$\Gamma(\rho^0 \to \pi^0\gamma) = 121 \pm 31 \text{ keV,} \tag{18}$$

$$\Gamma(\omega \to \pi^0\pi^0\gamma) < 3.4 \text{ keV.} \tag{19}$$

Here and further the total errors are shown, including both statistical and systematic ones.

In the case of the decays (3) and (4) it is not possible to choose the unique solution (see Table 2) using experimental data, so we present both solutions:

1) for constructive $\rho - \omega$ interference

$$B(\omega \to \eta\gamma) = (7.3 \pm 2.9) \cdot 10^{-4},$$
$$B(\rho \to \eta\gamma) = (4.0 \pm 1.1) \cdot 10^{-4},$$

$$\Gamma(\omega \to \eta\gamma) = 6.1 \pm 2.5 \text{ keV,}$$
$$\Gamma(\rho \to \eta\gamma) = 62 \pm 17 \text{ keV;}$$

2) for destructive $\rho - \omega$ interference

$$B(\omega \to \eta\gamma) = (3.5 \pm 0.5) \cdot 10^{-3},$$
$$B(\rho \to \eta\gamma) = (7.3 \pm 1.5) \cdot 10^{-4},$$

$$\Gamma(\omega \to \eta\gamma) = 29.4 \pm 4.7 \text{ keV,}$$
$$\Gamma(\rho \to \eta\gamma) = 111 \pm 22 \text{ keV.}$$

It should be mentioned that the negative sign of $\rho - \omega$ interference and the widths obtained under this assumption contradict the quark model, well confirmed in all other measured radiative decays of light vector mesons.

8. CONCLUSION

The branching ratios $B(\omega \to \pi^+\pi^-\pi^0)$, $B(\omega \to \pi^0\gamma)$ and $B(\omega \to e^+e^-)$ obtained in this work agree well with the world averages presented in [3]. Their errors are also close to world average, but to compare this experiment with the most precise of previous ones [15], the former has two times smaller error of $B(\omega \to \pi^0\gamma)$ than the latter. The partial widths of all decay modes of ω meson turned out to be smaller than its table values by 15% in average due to new and more accurate measurement of the width of ω meson [13].

$B(\rho^0 \to \pi^0\gamma)$ has been measured for the first time. The value is in agreement with the previous measurement of $B(\rho^- \to \pi^-\gamma)$ with the use of Primakoff-effect [6].

The strong evidence has been obtained for constructive $\rho - \omega$ interference in $\pi^0\gamma$ decay.

The branching ratios $B(\rho \to \eta\gamma)$ and $B(\omega \to \eta\gamma)$ obtained in this work confirm the only previous measurement in diffractive photo-production of ρ and ω mesons [4], but the accuracy has not been improved significantly.

The upper limit of the branching ratio of the decay $\omega \to \pi^0\pi^0\gamma$ was lowered by more than one order of magnitude.

The results obtained with the Neutral Detector for radiative decays of $\rho, \omega, \Phi \to \pi^0\gamma, \eta\gamma$ agree well with the predictions of quark model for the parameters evaluated from the formulae for masses of mesons and magnetic moments of barions [2]. The differences between experimental values and theoretical predictions are less than 10% and are consistent with an experimental accuracy. To ascertain the parameters of the model itself the more detailed information is needed on overlap integrals and difference of magnetic moments of quarks in mesons and barions. The experimental accuracy should be also improved.

REFERENCES

1. *Azimov Ja.I. et al.*, Pisma v JETP, V.1, No.2 (1965) 50—54;
   Anisovich V.V. et al., Phys. Lett., V.16, No.2 (1965) 194.
2. *O'Donnel P.*, Rev. Mod. Phys., V.53, No.4 (1981) 673.
3. Particle Data Group, Phys. Lett., B170 (1986).
4. *Andrews D.E. et al.*, Phys. Rev. Lett., V.38 (1977) 198.
5. *Jensen T. et al.*, Phys. Rev., D27 (1983) 26.
6. *Cappraro L. et al.*, Nucl. Phys., B288 (1987) 659.
7. *Druzhinin V.P. et al.*, Phys. Lett., 144B (1984) 136.
8. *Druzhinin V.P. et al.*, Z. Phys. C, 37 (1987) 1.
9. *Tumaikin G.M.*, Proceedings of the 10-th International Conference on High Energy Particle Accelerators, Serpukhov, 1977, V.1, p.443.
10. *Golubev V.B. et al.*, Nucl. Instr. and Methods, 227 (1984) 467.
11. *Berge J. et al.*, Rev. Sci. Instr., 32 (1961) 538.
12. *Achasov N.N., Shestakov G.N.*, Elem. Chast. i At. Jadra, V.9, No.1 (1978) 48.
13. *Aulchenko V.M. et al.*, Phys .Lett., B186 (1987) 432.
14. *Vasserman I.B. et al.*, Pisma v JETP, V.44, No.11 (1986) 493.
15. *Keyne J. et al.*, Phys. Rev., D14 (1976) 28.

S.I.Dolinsky, V.P.Druzhinin, M.S.D.. rovin,
V.B.Golubev, V.N.Ivanchenko, A.P.Lysenko,
A.A.Mikhailichenko, E.V.Pakhtusova, A.N.Peryshkin,
S.I.Serednyakov, Yu.M.Shatunov, V.A.Sidorov

Radiative Decays of ρ and ω Mesons

В.Б. Голубев, С.И. Долинский, В.П. Дружинин,
М.С. Дубровин, В.Н. Иванченко, А.П. Лысенко,
А.А. Михайличенко, Е.В. Пахтусова, А.Н. Перышкин,
С.И. Середняков, В.А. Сидоров, Ю.М. Шатунов

Радиационные распады ρ- и ω-мезонов